Egypt. J. Chem. **Vol. 67,** No. 10 pp. 181 -189 (2024)

Egyptian Journal of Chemistry

http://ejchem.journals.ekb.eg/

An Investigation of Structural, Electrical and Optical Properties of Metal Free-Zinc Oxide Thin Films Using Spray Pyrolysis Sol-Gel Techniques

Salah Eddine Boussaada [a], Younes Mouchaal [a,b*], Houaria Riane [a], Abdelbacet Khelil [b]

[a] *Faculty of Exacte Sciences, Mustapha Stambouli Mascara University, Algeria.*
[b] *LPCMME Lab, Faculty of Exacte and applied Sciences, University Oran 1 Ahmed Ben Bella, Algeria*

Abstract

Zinc oxide (ZnO) has garnered significant attention in recent years for its outstanding properties in the realm of transparent electronics, notably its substantial direct bandgap (Eg). This study focuses on the fabrication of pure ZnO thin films via the Spray pyrolysis Deposition technique on glass substrates. By adjusting both concentration and spray cycles during deposition, a comprehensive analysis of the resulting films structural, optical, morphological, and electrical characteristics was conducted. Notably, promising outcomes were achieved leading to transparent and high conductive structure without the need for metal doping. Most performant result were obtained using structure from 0.04 mole solution, yielding an optical transparency of 60.55%, electrical conductivity of 20.6 $\Omega^{-1}cm^{-1}$, a mobility of 5.87 cm^2/Vs, and an optical bandgap of 3.50 eV. Structural analysis performed via XRD showed hexagonal polycrystalline Wurtzite structure with favored (002) orientation. These findings suggest that ZnO thin films hold the potential for applications in optoelectronic devices.

Keywords: ZnO, Spray Pyrolysis, Hall Effect measurements, Wurtzite structure, Mobility

1. Introduction

Materials known as transparent conducting oxides (TCOs) have strong electrical conductivity as well as optical transparency [1]. These substances find frequent applications in electronic gadgets like flat-panel screens, touchscreen interfaces, and photovoltaic cells, where their indispensable qualities include efficient electrical conduction and the transmission of light [2]. The most commonly used TCOs are metal oxides, such as indium tin oxide (ITO), which is widely used in commercial applications [3,4]. Other examples of TCOs include un-doped and fluorine-doped tin oxide (SnO_2-FTO), un-doped and aluminum-doped zinc oxide (ZnO-AZO) [5,6].

Zinc oxide (ZnO) is a semiconductor material with a broad bandgap of 3.38 eV and a variety of intriguing optical characteristics [7], including substantial ultraviolet absorption and high transparency in the visible part of the electromagnetic spectrum [8]. It is highly transparent to visible light, with a transparency of up to 90% in the visible spectrum [9]. This makes it an ideal material for use in applications where transparency is important, such as in display technologies. ZnO has a high exciton binding energy at 60 meV [10,11], or the amount of power needed to split an electron from a hole in the substance. ZnO structures are highly effective at absorbing ultraviolet (UV) radiation, with a strong absorption peak at around 370 nm. Near the absorption edge, a clear exciton peak can be seen, indicating that ZnO has a high degree of crystalline quality [12,13]. When excited by light, ZnO emits light at a specific wavelength, a property known as photo-luminescence. Due to this characteristic, it is a desirable material for solar cells (SC), light-emitting diodes (LEDs), and sunscreens, among other optoelectronic devices [14]. Most of the studies concerning ZnO-based electrodes have been documented in relation to inorganic solar cells (ISC) [15].

Zinc oxide is classified as an n-type semiconductor and is commonly chosen as the window layer for solar cells [16]. These unique properties of ZnO make it an excellent candidate for use as a TCO [17]. Several methods, including Pulsed Laser Deposition [18–20], Sol-gel [20–24], Radio Frequency (RF) Magnetron Sputtering [25], Vapor Deposition (CVD) [26], and Spray Pyrolysis Deposition (SPD) [27]. It has been used to

*Corresponding author e-mail: younes.mouchaal@univ-mascara.dz; (Younes Mouchaal)
Receive Date: 30 January 2024, Revise Date: 01 March 2024, Accept Date: 18 April 2024
DOI: 10.21608/ejchem.2024.266541.9265

manufacture ZnO thin films. SPD was first created for the deposition of TCO material for SC, as opposed to conventional deposition processes [28].

This study aims to introduce the SPD synthesis technique for producing transparent and conductive ZnO thin films and investigate the impact of two different solution concentrations on their morphology, structural properties, and photoelectric characteristics. The main objective lies in obtaining highly conductive structures without using metal doping, which makes it possible to facilitate the deposition procedures and considerably reduce the cost of manufacturing such structures.

2. Materials and methods

Precursor solution preparation and thin films deposition

Two solutions containing zinc chloride ($ZnCl_2$) with two molar concentrations of 0.04 mol/l and 0.02 mol/l were prepared in methanol (CH_3OH) as solvent. We name (A) the solution of molar concentration 0.04 mol/l, and (B) the solution of 0.02 mol/l. To achieve complete elemental dissolution and prevent compound precipitation, which could negatively impact the morphology of the thin films to be deposited, precursor solutions A and B were agitated using a magnetic stirrer at a low speed at a temperature of 60°C for 20 minutes. To solutions A and B, 0.7 ml of HCl is added while the mixture is being stirred. It's important to note that the gas-phase breakdown of $ZnCl_2$ on the substrate surface is an endothermic reaction, requiring elevated temperatures for the decomposition (pyrolysis) of the solutions (droplets) applied to heated substrates.

This chemical reaction can be summarized by an equation (1):

$$ZnCl_{2\,(g)} + CH_3OH_{(cl)} + O_2 \rightarrow ZnO_{(s)} + 2HCl_{(g)} + CO_{2\,(g)} + H_{2\,(g)} \quad (1)$$

The two prepared solutions were sprayed glass substrates (MICRO SOLID, ISOLAB GERMANY®) with highly controlled mechanical, optical and morphological properties of the brand with dimensions of 15 x 25 mm.

According to literature and research, the resulting thin films were annealed at a temperature of 400 °C [29,30]. The heat treatment has an important effect on the optical and electrical properties of the deposited ZnO layers ensuring reorganization of the structure allowing the removal of residual impurities and defects in the ZnO [31,32]. The deposition parameters of ZnO thin films at different concentrations (A and B) and cycle numbers (C= 20, 30 and 40) are summarized in Table 1.

Table 1 Thin films deposition parameters via spray pyrolysis root.

Deposition parameters	Values
Concentration of the solution	A: 0.04 M and B: 0.02 M
Precursors	$ZnCl_2$:H_2O
Solvent	CH_3OH
Substrate temperature	400±5 °C
Transport gas	Compressed Air (1.2 bar)
Substrate-atomizer distance	25 cm
Spray speed	28 ±1 ml/min
Number of cycles	varied: 2, 3 and 4
Number of sequences for each cycle	10
Spray time per sequence	45 s
Pause between sequences	30 s

Thin films Characterization

The conductivity (σ), mobility (μ) and resistivity (ρ) were calculated by the Hall Effect measurement system ECOPIA (HMS 1000).

Optical transmission measurements within the UV-Visible range (300-800 nm) were conducted using a Perkin-Elmer Lambda 950 UV-Vis-NIR spectrophotometer equipped with an integrating sphere. The measurements were carried out at a scanning rate of 60 nm/min.

The thin film thickness measurements were conducted using a mechanical profilometer, specifically the Bruker Dektak XT instrument.

XRD was used to determine the structural characteristics of the thin films (Rigaku-Miniflex 600) using Cu Kα X-radiation (λ = 1.5405 Å) in the range 2θ = 20° to 80° with a measurement step of 0.10.

The surface's morphology and microstructure were examined using a scanning electron microscope (SEM-JOEL JSM-6610La from Japan), incorporating an energy dispersive X-ray analysis (EDX) system for further analysis.

3. Resultant and discussion

Electrical study

Table 2 presents the variations in electrical conductivity concerning changes in concentration and the number of deposition cycles. It illustrates a notable decline in electrical conductivity for ZnO films as the number of cycles increases in both solutions despite C3 samples from solutions A. This study shows that best electrical performances of ZnO thin films can be obtained using considerably low concentration precursor solution with long time deposition. The decline in conductivity is attributed to a rise in oxidation, as prior research has shown that when cycles increase, the amount of oxygen also increases [33].

Table 2 Electrical parameters of ZnO spray pyrolysis thin films annealing of 1h - 400°C.

Solution	Number of cycles	σ $(\Omega\ cm)^{-1}$	ρ (Ω cm)	μ (cm^2/Vs)
A	C1	20.6	4.85×10^{-2}	5.87
	C2	1.04	0.96	0.266
	C3	7.98×10^{2}	1.25×10^{-3}	1.14×10^{3}
B	C1	49.8	$2\ 10^{-2}$	11
	C2	40.2	2.48×10^{-2}	6.82
	C3	1.26	0.79	0.6

Optical study

The optical properties of transparent electrodes are important in the reliability of optoelectronic devices, where they are supposed to transmit the maximum of the incident light spectrum to the active layers of the device in which they are integrated**.** We were interested in optical transmission measurements in the visible-near UV and IR regions as a function of light energy. The optical transmission spectrum of ZnO thin films derived from two solutions, and after varying numbers of cycles is displayed in the forthcoming Figure 1. From the transmission spectra of the ZnO layers we can see that the transmission varies with concentration and number of cycles. The average transmission decreases linearly with increasing concentration and number of spray deposition cycles. According to the Beer-Lambert equation [34], which shows that the inversely proportional relationship between optical transmission and thickness is as follows [35], this finding can be explained by the fact that the film thickness increases as the number of cycles increases.

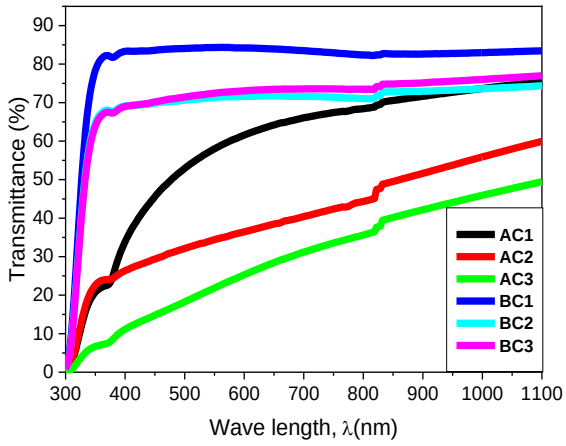

Fig 1: Optical transmittance of ZnO thin films

Table 3 Optical properties of the processed ZnO samples

Sample	$\bar{T}$ (400-800)	$\bar{T}$ (300-1100)	T_{max} (%)	λ_{max} (nm)
AC1	60.55	62.12	75.18	1100
BC1	83.68	80.62	84.42	600

The results showed that the samples with the least number of cycles (20 cycles), AC1 and BC1, are the thinnest and most transparent, and this is supported by many other research studies [36–38]

The Tauc relation was used to calculate the optical bandgap energy for the relevant samples [39].

$$(\alpha h\upsilon)^n = B(h\upsilon - E_g) \quad (2)$$

E_g: optical gap energy

α: absorption coefficient

B: constant

hυ: energy of the incident photon.

We have also used the mathematical formula:

$$E = \frac{h.c}{\lambda} \quad (3)$$

Where *h* is Plank's constant, *c* is the speed of light, and λ is the absorption wavelength.

In Figure 2, the variation of the entity $(\alpha h\upsilon)^2$ as a function of the photon energy $(h\upsilon)$ and extrapolated the linear part of the curve and the intersection with the x-axis (the point of the intersection between the linear part and the x-axis), we then deduced the gap energy values which are grouped in Table 4. The band gap energy of the ZnO thin films was greater than the average band gap energy of Eg = 3.26 eV reported for single crystal ZnO [40]. This figure agrees with the previously published value of Eg = 3.33 eV for Cobalt-doped ZnO films [41]. Nonetheless, as the thickness of the film increased, there was a notable reduction in the optical bandgap energy of the ZnO thin film (see Table 4). This drop was ascribed to changes in barrier height caused by crystallite size changes in polycrystalline films.

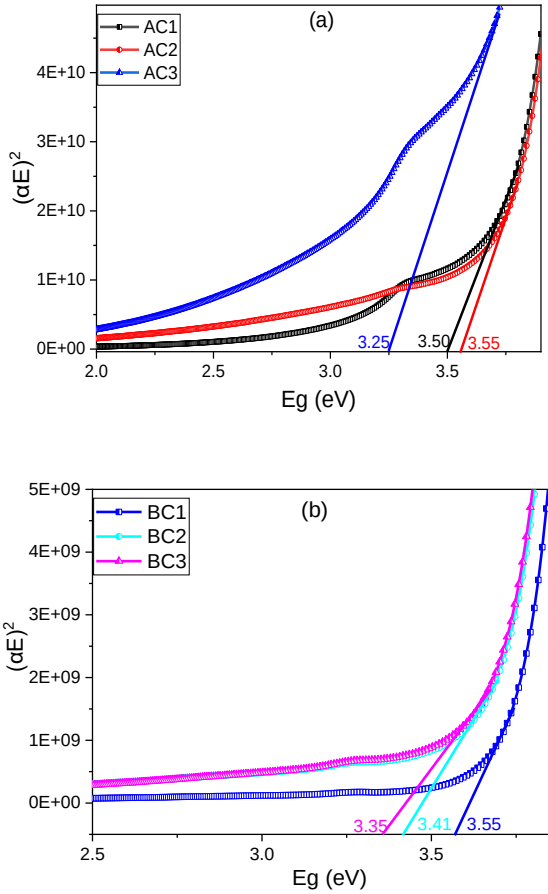

Fig 2: The $(\alpha h\upsilon)^2$ versus photon energy curves of ZnO thin films deposited with different spray cycles: (a): from solution A and (b): from solution B

Table 4 Bandgap and thickness values of spray pyrolysis deposited ZnO Thin films.

sample	AC1	AC2	AC3	BC1	BC2	BC3
bandgap (eV)	3.50	3.55	3.25	3.55	3.41	3.35
Thickness (µm)	0.44	0.82	1.0	1.30	1.79	1.81

Figure 3 shows the evolution of deposited pure ZnO thin films thickness carried out employing a mechanical Profilometer. We notice an increase in the thickness of the ZnO thin films as a function of the number of spraying cycles. The ZnO film growth appears to be directly proportional to the number of sputtering cycles. The line of the best fit doesn't intersect with the origin, suggesting that there's a period of incubation during the initial stages of growth, where the grains merge and develop into the thin ZnO film. This period for nucleation/coalescence is commonly observed in spray pyrolysis procedures[42,43]. Based on this calibration, it was determined those 20 sputtering cycles (AC1) corresponds to a ZnO thickness of approximately 440 nm, which is a typical value for use in TCO solar cells.

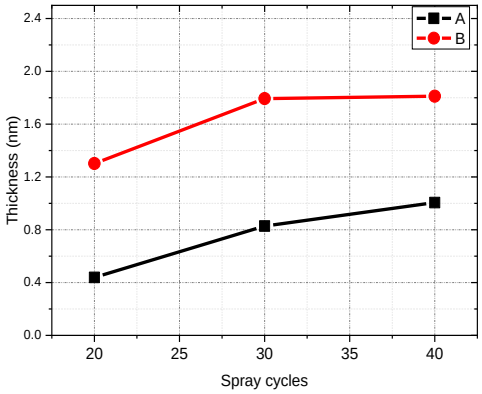

Fig 3: The relationship between the thickness of the ZnO film and the two concentrations and the number of spraying cycles

Structural Study

In order to investigate the crystalline nature of the oxide films generated, we opted for sample C1 from solution AC1 (0.04 mol) for X-ray diffraction (XRD) assessment.

Figure 4 depicts the XRD pattern obtained in an acquisition time set to 30 minutes, utilizing grazing incidence. The XRD pattern reveals seven distinct diffraction peaks in the ZnO thin film (AC1) at angles of 31.38°, 34.29°, 36.03°, 47.39°, 56.44°, 62.50° and 67.97°, corresponding to the (100), (002), (101), (102), (110), (103) and (112) crystallographic planes, respectively. The XRD of the ZnO film indicates its polycrystalline nature, adhering to the hexagonal Wurtzite structure (Zincite Phase JCPDS 36-1451) [44,45]. Additionally, it exhibits a preferential orientation with the substrate aligned perpendicular to the c-axis.

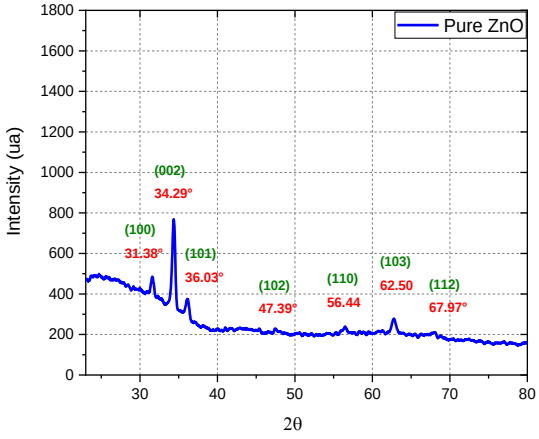

Fig 4: X-ray diffraction pattern as a function of 2θ of ZnO thin films (AC1)

For more insight into these structural modifications of the pure ZnO thin film, the mesh parameters "a" and "c," along with the unit cell volume "V," are calculated based on the Bragg relation[46] and utilizing the following formula: [47,48]

$$2d_{hkl}\ sin\theta = \lambda n \quad (4)$$

$$\frac{1}{d_{hkl}^2} = \frac{4(hk+h^2+k^2)}{3a^2} + \frac{l^2}{c^2} \quad (5)$$

$$V = a^2 c \quad (6)$$

The variables d_{hkl} and n represent the inter-reticular distance and diffraction order (0,1,2…), respectively. The computed lattice parameters values are quite near to the values a = 0.32503 nm and c = 0.52074 nm for pure and stoichiometric ZnO derived from the RRUFF database, as shown in the table 5.

The Deby-Schrrer formula [49], which is used a lot, was used to find the crystallite grain size (D) for the pure ZnO thin film. For the calculation, the numbers for the most intense peak of (002), (100), and (101) had to be found. The outcomes of this analysis are illustrated in table 5.

$$D = \frac{0.9\lambda}{\beta \cos\theta} \quad (7)$$

The equation involves the variables D, β, θ, and λ, which respectively indicate the average size of the crystallite, the full width half maximum (FWHM) measured in radians, Bragg's angle, and the wavelength of X-rays. The acquired results suggest that the crystalline grain size of pure ZnO thin film stands at an estimated 20.78 nm at (002), a value that appears to be reasonable when juxtaposed with findings from other studies conducted in this research domain (table 5) [50].

Micro-strain (ε) is a crucial attribute in nanostructured thin films, arising from crystalline imperfections that alter lattice constants. The strain (ε) and density of dislocations (δ) in the thin films were determined using the formulae [51,52]:

$$\varepsilon = \frac{\beta cos\theta}{4} \quad (8)$$

$$\delta = \frac{1}{D^2} \quad (9)$$

The calculated value of ε and δ are shown in Table 5. Pure ZnO at (002) gave values of ε and δ, which were determined to be 9.55 and 2.314, respectively.

Morphological study

We present in figure 5 the images obtained by Scanning Electron Microscope of the Spray Pyrolysis.

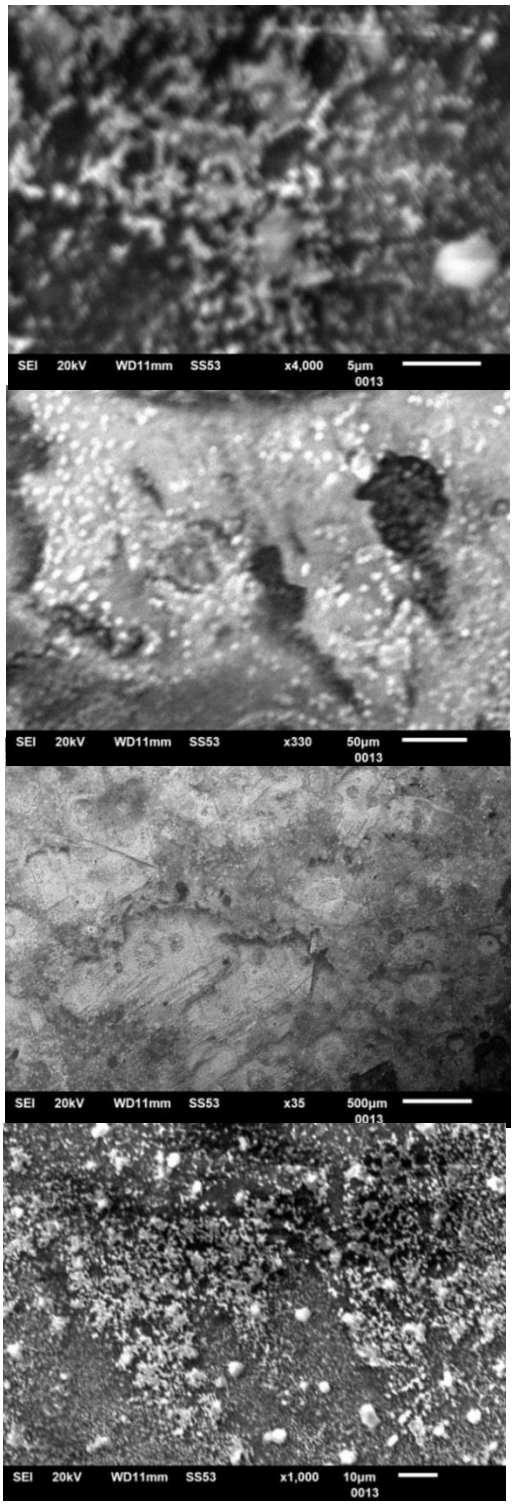

Fig 5: SEM image of pure ZnO (AC1) spray pyrolysis thin films

Indeed, the surface morphology of the sample (AC1) seen by SEM shows roughness formed by grains of average size (~~50 nm~~ (between 20 and 25 nm) randomly distributed on the substrate surface.

Elemental Analysis

Energy dispersive X-ray (EDX) analysis was employed to investigate the elemental composition of the ZnO thin films. The corresponding results are detailed in Figure 6. From the results obtained we confirm the composition of our sample with the inspected presence of Zn and O peaks, the other elements observed belong to the elements of the composition of the glass substrate (Si, Mg, C, Al....) as the EDX analysis has a certain depth of analysis given by the depth of escape of the RX emitted as a result of the electronic impact. The EDX results show an excess of oxygen in the elementary evaluation due to the OH sites adsorbed on the surface of the ZnO films given that the analysis is carried out at ambient conditions in open air.

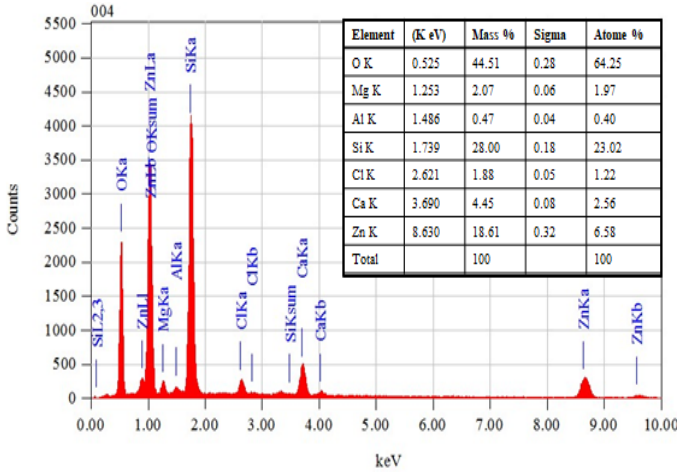

Fig 6: The result of EDX analysis of ZnO films deposited by Spray pyrolysis

Table 5 Structural parameters and crystallite size of pure ZnO thin films

Pure ZnO (hkl)	2θ (°)	Intensity (a.u)	FWHM (°)	d(hkl)	crystallites size D (nm)	Strain ε ×10^{-3}	dislocation density δ× 10^{15} (line/m^2)	Lattice parameters a (Å)	c (Å)	Cell volume V (Å^3)
(100)	31.59	38.99	0.36	0.2829	23.06	1.50	1.880	3.2677	5.2172	55.7085
(002)	34.35	226.57	0.40	0.2608	20.78	1.60	2.314			
(101)	36.11	30.62	0.35	0.2485	23.87	1.45	1.755			
[50]	34.57	-	0.054	-	26.59	1.30	1.413	3.23	5.19	

4. Conclusion

In this study, we fabricated pure ZnO thin film using the Spray Pyrolysis (SPD) method for potential photovoltaic applications. The resulting film AC1 exhibited a hexagonal wurtzite structure with a transmittance exceeding 60.55% in the visible spectrum and bandgap energy of 3.50 eV. Notably, the film demonstrated a low resistivity of 4.85 10^{-2} Ω cm, an electron mobility of 5.87 cm^2/Vs, and a thickness of 440 nm. When compared to different levels of ZnO, films created by the spray pyrolysis method provide reliable performance for optoelectronic devices.

This experimental approach has shown the possibility of developing structures presenting considerable transparency and electrical conductivity compromises without resorting to metallic doping.

These results pave the way for the development of structures and stable devices while avoiding the damage caused by the presence of doping elements characterized by diffusion within the structures. This approach also promotes the manufacturing of cost effective devices by avoiding the consumption of metallic elements and the simplification of manufacturing processes.

Reference

[1] M. Hadjab, O. Guskova, H. Bennacer, M.I. Ziane, A.H. Larbi, M.A. Saeed, Ground-state properties of p-type delafossite transparent conducting oxides 2H-CuMO2 (M=Al, Sc and Y): DFT calculations, Materials Today Communications 32 (2022) 103995.

https://doi.org/10.1016/j.mtcomm.2022.103995.

[2] J. Ajayan, D. Nirmal, P. Mohankumar, M. Saravanan, M. Jagadesh, L. Arivazhagan, A review of photovoltaic performance of organic/inorganic solar cells for future renewable and sustainable energy technologies, Superlattices and Microstructures 143 (2020) 106549. https://doi.org/10.1016/j.spmi.2020.106549.

[3] O. Tuna, Y. Selamet, G. Aygun, L. Ozyuzer, High quality ITO thin films grown by dc and RF sputtering without oxygen, J. Phys. D: Appl. Phys. 43 (2010) 055402. https://doi.org/10.1088/0022-3727/43/5/055402.

[4] H. Koseoglu, F. Turkoglu, M. Kurt, M.D. Yaman, F.G. Akca, G. Aygun, L. Ozyuzer, Improvement of optical and electrical properties of ITO thin films by electro-annealing, Vacuum 120 (2015) 8–13. https://doi.org/10.1016/j.vacuum.2015.06.027.

[5] H.Z. Asl, S.M. Rozati, High-Performance Spray-Deposited Indium Doped ZnO Thin Film: Structural, Morphological, Electrical, Optical, and Photoluminescence Study, J. Electron. Mater. 47 (2018) 3568–3576. https://doi.org/10.1007/s11664-018-6201-1.

[6] S.V.N. Pammi, A. Chanda, N.-J. Seong, S.-G. Yoon, Growth of high-quality ITO thin films at low temperature by tuning the oxygen flow rate using the nano-cluster deposition (NCD) technique, Chemical Physics Letters 490 (2010) 234–237. https://doi.org/10.1016/j.cplett.2010.03.035.

[7] N. Padha, Growth of ZnO 2D layers by Atomic Layer Deposition (ALD) and study of its physical properties for photovoltaic and photoconvertor device applications, SPAST Abstracts 1 (2021). https://spast.org/techrep/article/view/2290 (accessed January 22, 2024).

[8] S. Tarasi, A. Morsali, Fabrication of transparent ultraviolet blocking films using nanocomposites derived from metal-organic frameworks, Journal of Alloys and Compounds 868 (2021) 158996. https://doi.org/10.1016/j.jallcom.2021.158996.

[9] L. Huang, T. Wang, X. Li, X. Wang, W. Zhang, Y. Yang, Y. Tang, UV-to-IR highly transparent ultrathin diamond nanofilms with intriguing performances: Anti-fogging, self-cleaning and self-lubricating, Applied Surface Science 527 (2020) 146733. https://doi.org/10.1016/j.apsusc.2020.146733.

[10] Y. Cheng, X. Zhang, L. Che, J. Chen, B. Jing, R. Sun, X. Luo, Binding energy of Sb-related complex in p-doped ZnO film, Journal of Alloys and Compounds 800 (2019) 219–223. https://doi.org/10.1016/j.jallcom.2019.06.033.

[11] T.S. Bjørheim, S. Erdal, K.M. Johansen, K.E. Knutsen, T. Norby, H and Li Related Defects in ZnO and Their Effect on Electrical Properties, J. Phys. Chem. C 116 (2012) 23764–23772. https://doi.org/10.1021/jp307835c.

[12] A. Janotti, C.G.V. de Walle, Fundamentals of zinc oxide as a semiconductor, Rep. Prog. Phys. 72 (2009) 126501. https://doi.org/10.1088/0034-4885/72/12/126501.

[13] Y. Chen, D.M. Bagnall, H. Koh, K. Park, K. Hiraga, Z. Zhu, T. Yao, Plasma assisted molecular beam epitaxy of ZnO on c -plane sapphire: Growth and characterization, Journal of Applied Physics 84 (1998) 3912–3918. https://doi.org/10.1063/1.368595.

[14] I. Ayoub, V. Kumar, R. Abolhassani, R. Sehgal, V. Sharma, R. Sehgal, H.C. Swart, Y.K. Mishra, Advances in ZnO: Manipulation of defects for enhancing their technological potentials, Nanotechnology Reviews 11 (2022) 575–619. https://doi.org/10.1515/ntrev-2022-0035.

[15] A.B. Djurišić, X. Liu, Y.H. Leung, Zinc oxide films and nanomaterials for photovoltaic applications, Physica Status Solidi (RRL) – Rapid Research Letters 8 (2014) 123–132. https://doi.org/10.1002/pssr.201300103.

[16] J. Sultana, S. Paul, R. Saha, S. Sikdar, A. Karmakar, S. Chattopadhyay, Optical and electronic properties of chemical bath deposited p-CuO and n-ZnO nanowires on silicon substrates: p-CuO/n-ZnO nanowires solar cells with high open-circuit voltage and short-circuit current, Thin Solid Films 699 (2020) 137861. https://doi.org/10.1016/j.tsf.2020.137861.

[17] C. Otalora, M.A. Botero, G. Ordoñez, ZnO compact layers used in third-generation photovoltaic devices: a review, J Mater Sci 56 (2021) 15538–15571. https://doi.org/10.1007/s10853-021-06275-5.

[18] W. Zhao-yang, H. Li-zhong, Z. Jie, S. Jie, W. Zhi-jun, Effect of the variation of temperature on the structural and optical properties of ZnO thin films prepared on Si (111) substrates using PLD, Vacuum 78 (2005) 53–57. https://doi.org/10.1016/j.vacuum.2004.12.014.

[19] X.W. Sun, H.S. Kwok, Optical properties of epitaxially grown zinc oxide films on sapphire by pulsed laser deposition, Journal of Applied Physics 86 (1999) 408–411. https://doi.org/10.1063/1.370744.

[20] H. Cao, J.Y. Wu, H.C. Ong, J.Y. Dai, R.P.H. Chang, Second harmonic generation in laser ablated zinc oxide thin films, Applied Physics

Letters 73 (1998) 572–574. https://doi.org/10.1063/1.121859.
[21] P. Misra, L.M. Kukreja, Buffer-assisted low temperature growth of high crystalline quality ZnO films using Pulsed Laser Deposition, Thin Solid Films 485 (2005) 42–46. https://doi.org/10.1016/j.tsf.2005.03.014.
[22] E.F. Keskenler, M. Tomakin, S. Doğan, G. Turgut, S. Aydın, S. Duman, B. Gürbulak, Growth and characterization of Ag/n-ZnO/p-Si/Al heterojunction diode by sol–gel spin technique, Journal of Alloys and Compounds 550 (2013) 129–132. https://doi.org/10.1016/j.jallcom.2012.09.131.
[23] F. Khan, S.-H. Baek, J.H. Kim, Influence of Ag doping on structural, optical, and photoluminescence properties of nanostructured AZO films by sol–gel technique, Journal of Alloys and Compounds 584 (2014) 190–194. https://doi.org/10.1016/j.jallcom.2013.09.055.
[24] G. Turgut, S. Duman, E.F. Keskenler, The influence of Y contribution on crystallographic, topographic and optical properties of ZnO: A heterojunction diode application, Superlattices and Microstructures 86 (2015) 363–371. https://doi.org/10.1016/j.spmi.2015.08.002.
[25] M. Selmi, F. Chaabouni, M. Abaab, B. Rezig, Studies on the properties of sputter-deposited Al-doped ZnO films, Superlattices and Microstructures 44 (2008) 268–275. https://doi.org/10.1016/j.spmi.2008.06.005.
[26] G.H. Lee, Y. Yamamoto, M. Kourogi, M. Ohtsu, Blue shift in room temperature photoluminescence from photo-chemical vapor deposited ZnO films, Thin Solid Films 386 (2001) 117–120. https://doi.org/10.1016/S0040-6090(01)00764-7.
[27] S. Yılmaz, E. McGlynn, E. Bacaksız, J. Cullen, R.K. Chellappan, Structural, optical and magnetic properties of Ni-doped ZnO micro-rods grown by the spray pyrolysis method, Chemical Physics Letters 525–526 (2012) 72–76. https://doi.org/10.1016/j.cplett.2012.01.003.
[28] N. Guermat, W. Daranfed, I. Bouchama, N. Bouarissa, Investigation of structural, morphological, optical and electrical properties of Co/Ni co-doped ZnO thin films, Journal of Molecular Structure 1225 (2021) 129134. https://doi.org/10.1016/j.molstruc.2020.129134.
[29] N. Guermat, W. Daranfed, K. Mirouh, Extended Wide Band Gap Amorphous ZnO Thin Films Deposited by Spray Pyrolysis, Annales de Chimie Science Des Matériaux 44 (2020) 347–352. https://doi.org/10.18280/acsm.440507.
[30] A.A. Aboud, M. Al-Dossari, N.S. AbdEL-Gawaad, A. Magdi, Effect of annealing onto physical properties of Co:ZnO thin films prepared by spray pyrolysis technique, Phys. Scr. 98 (2023) 095958. https://doi.org/10.1088/1402-4896/acf167.
[31] W.C. Lim, J.P. Singh, Y. Kim, J. Song, K.H. Chae, T.-Y. Seong, Effect of thermal annealing on the properties of ZnO thin films, Vacuum 183 (2021) 109776. https://doi.org/10.1016/j.vacuum.2020.109776.
[32] S. Kurtaran, Al doped ZnO thin films obtained by spray pyrolysis technique: Influence of different annealing time, Optical Materials 114 (2021) 110908. https://doi.org/10.1016/j.optmat.2021.110908.
[33] V.L. Patil, S.A. Vanalakar, P.S. Patil, J.H. Kim, Fabrication of nanostructured ZnO thin films based NO2 gas sensor via SILAR technique, Sensors and Actuators B: Chemical 239 (2017) 1185–1193. https://doi.org/10.1016/j.snb.2016.08.130.
[34] T.G. Mayerhöfer, S. Pahlow, J. Popp, The Bouguer-Beer-Lambert Law: Shining Light on the Obscure, ChemPhysChem 21 (2020) 2029–2046. https://doi.org/10.1002/cphc.202000464.
[35] R.A. Zargar, K. Kumar, Z.M.M. Mahmoud, M. Shkir, S. AlFaify, Optical characteristics of ZnO films under different thickness: A MATLAB-based computer calculation for photovoltaic applications, Physica B: Condensed Matter 631 (2022) 413614. https://doi.org/10.1016/j.physb.2021.413614.
[36] G. Yergaliuly, B. Soltabayev, S. Kalybekkyzy, Z. Bakenov, A. Mentbayeva, Effect of thickness and reaction media on properties of ZnO thin films by SILAR, Sci Rep 12 (2022) 851. https://doi.org/10.1038/s41598-022-04782-2.
[37] S. Gao, X. Zhao, Q. Fu, T. Zhang, J. Zhu, F. Hou, J. Ni, C. Zhu, T. Li, Y. Wang, V. Murugadoss, G.A.M. Mersal, M.M. Ibrahim, Z.M. El-Bahy, M. Huang, Z. Guo, Highly transmitted silver nanowires-SWCNTs conductive flexible film by nested density structure and aluminum-doped zinc oxide capping layer for flexible amorphous silicon solar cells, Journal of Materials Science & Technology 126 (2022) 152–160. https://doi.org/10.1016/j.jmst.2022.03.012.
[38] A.M. Shehabeldine, A.H. Hashem, A.R. Wassel, M. Hasanin, Antimicrobial and Antiviral Activities of Durable Cotton Fabrics Treated with Nanocomposite Based on Zinc Oxide Nanoparticles, Acyclovir, Nanochitosan, and Clove Oil, Appl Biochem Biotechnol 194 (2022) 783–800. https://doi.org/10.1007/s12010-021-03649-y.

[39] M.K. Hossain, D.P. Samajdar, R.C. Das, A.A. Arnab, Md.F. Rahman, M.H.K. Rubel, Md.R. Islam, H. Bencherif, R. Pandey, J. Madan, M.K.A. Mohammed, Design and Simulation of Cs2BiAgI6 Double Perovskite Solar Cells with Different Electron Transport Layers for Efficiency Enhancement, Energy Fuels 37 (2023) 3957–3979. https://doi.org/10.1021/acs.energyfuels.3c00181.

[40] R. Mimouni, O. Kamoun, A. Yumak, A. Mhamdi, K. Boubaker, P. Petkova, M. Amlouk, Effect of Mn content on structural, optical, opto-thermal and electrical properties of ZnO:Mn sprayed thin films compounds, Journal of Alloys and Compounds 645 (2015) 100–111. https://doi.org/10.1016/j.jallcom.2015.05.012.

[41] G. Marinov, B. Georgieva, M. Vasileva, T. Babeva, Study of Structure, Morphology and Optical Properties of Cobalt-Doped and Co/Al-co-Doped ZnO Thin Films Deposited by Electrospray Method, Applied Sciences 13 (2023) 9611. https://doi.org/10.3390/app13179611.

[42] A. Palafox, G. Romero-Paredes, A. Maldonado, R. Asomoza, D.R. Acosta, J. Palacios-Gomez, Physical properties of CdS and CdS:In thin films obtained by chemical spray over different substrates, Solar Energy Materials and Solar Cells 55 (1998) 31–41. https://doi.org/10.1016/S0927-0248(98)00044-0.

[43] K. Murakami, K. Nakajima, S. Kaneko, Initial growth of SnO2 thin film on the glass substrate deposited by the spray pyrolysis technique, Thin Solid Films 515 (2007) 8632–8636. https://doi.org/10.1016/j.tsf.2007.03.128.

[44] H.S. Rasheed, N.M. Ahmed, M.Z. Matjafri, F.A. Sabah, H.N. Al-Rawi, The Effect of the Annealing on the Properties of ZnO/Cu/ZnO Multilayer Structures, Procedia Chemistry 19 (2016) 38–44. https://doi.org/10.1016/j.proche.2016.03.011.

[45] Q. Sun, G. Li, T. Tian, Z. Man, L. Zheng, M. Barré, J. Dittmer, F. Goutenoire, A.H. Kassiba, Controllable microstructure tailoring for regulating conductivity in Al-doped ZnO ceramics, Journal of the European Ceramic Society 40 (2020) 349–354. https://doi.org/10.1016/j.jeurceramsoc.2019.10.011.

[46] M.E. Fragala, G. Malandrino, Characterization of ZnO and ZnO:Al films deposited by MOCVD on oriented and amorphous substrates, Microelectronics Journal 40 (2009) 381–384. https://doi.org/10.1016/j.mejo.2008.09.003.

[47] F. Hassan, M.S. Miran, H.A. Simol, M.H. Susan, M.Y.A. Mollah, Synthesis of ZnO nanoparticles by a hybrid electrochemical-thermal method: influence of calcination temperature, Bangladesh Journal of Scientific and Industrial Research 50 (2015) 21–28.

[48] Y. Zhao, Y. Li, W. Wan, X. Ren, H. Zhao, Surface defect and gas-sensing performance of the well-aligned Sm-doped SnO2 nanoarrays, Materials Letters 218 (2018) 22–26. https://doi.org/10.1016/j.matlet.2018.01.136.

[49] R. Zhang, M. Hummelgård, H. Olin, A facile one-step method for synthesising a parallelogram-shaped single-crystalline ZnO nanosheet, Materials Science and Engineering: B 184 (2014) 1–6. https://doi.org/10.1016/j.mseb.2013.12.009.

[50] K. Salim, W. Azzaoui, Physical properties of spray pyrolysed ZnO thin films obtained from nitrate, acetate and chloride precursors: Comparative study for Solar Cell Applications, Revista Mexicana de Física 69 (2023) 031002 1–8. https://doi.org/10.31349/RevMexFis.69.031002.

[51] M. Sathya, K. Pushpanathan, Synthesis and Optical Properties of Pb Doped ZnO Nanoparticles, Applied Surface Science 449 (2018) 346–357. https://doi.org/10.1016/j.apsusc.2017.11.127.

[52] K.E. Lee, M. Wang, E.J. Kim, S.H. Hahn, Structural, electrical and optical properties of sol–gel AZO thin films, Current Applied Physics 9 (2009) 683–687. https://doi.org/10.1016/j.cap.2008.06.006.